Force Field Design and Molecular Dynamics Simulations of the Carbapenem- and Cephamycin-Resistant Dinuclear Zinc Metallo-β-lactamase from *Bacteroides fragilis* and Its Complex with a Biphenyl Tetrazole Inhibitor

Hwangseo Park and Kenneth M. Merz, Jr.*

104 Chemistry Building, Department of Chemistry, Pennsylvania State University, University Park, Pennsylvania 16802-6300

Received October 29, 2004

On the basis of molecular dynamics simulations, we investigate the dynamic properties of the carbapenem- and cephamycin-resistant dinuclear zinc metallo-β-lactamase from *Bacteroides fragilis* and its complex with a biphenyl tetrazole inhibitor, 2-butyl-6-hydroxy-3-[2′-(1*H*-tetrazol-5-yl)biphenyl-4-ylmethyl]-3*H*-quinazolin-4-one **1** (L-159061). The results obtained with the newly developed force field parameters for the coordination environment of the catalytic zinc ions show that the active site gorge comprising major and minor loops gets deeper and narrower upon binding of the inhibitor, which supports the previous experimental implication that the structural flexibility of the loop structures plays a significant role in enzymatic action. In the presence of the inhibitor, the Trp32 side chain at the apex of the major loop covers the entrance of active site channel, thereby contributing to the stabilization of the enzyme−inhibitor complex. In addition to a direct coordination of the inhibitor tetrazole ring to the second zinc ion in the active site, the hydrogen bonding of Lys167 to the inhibitor carbonyl group and hydrophobic interactions between the inhibitor and side chains of loop residues prove to be significant binding forces of the enzyme−inhibitor complex.

Introduction

Bacterial resistance to β-lactam antibiotics stems from the expression of the β-lactamases that catalyze a hydrolytic cleavage of the substrate amidic bond. Of the four structural classes for these enzymes, metallo-β-lactamases (class B) contain zinc and other divalent cations in their active sites as cofactors for catalytic activity. Despite a relatively low population, broad substrate specificity and the absence of clinically useful inhibitors make pathogens with genes encoding this enzyme a hazard to human health. Therefore, a great deal of effort has been devoted to understanding structural and mechanistic features of metallo-β-lactamases from a variety of bacterial strains including, *Bacillus cereus*,[1−3] *Pseudomonas aeruginosa,*[4,5] *Stenotrophomonas maltophilia*,[6,7] and *Aeromonas hydrophila*.[8,9]

Due mainly to a high degree of catalytic activity against most classes of β-lactam antibiotics, the carbapenem- and cephamycin-resistant dizinc metallo-β-lactamase (CcrA) from *Bacteroides fragilis* has been most extensively studied so far. X-ray crystal structures were reported for both the apoenzyme[10,11] and its complex with competitive inhibitors.[12,13] The active site includes two zinc ions, both of which are required for full catalytic activity.[14] One zinc ion (Zn1) is coordinated to three histidine residues (His82, His84, His145)[15] and a bridging hydroxide ion (Wat1),[10] which is reminiscent of the carbonic anhydrase II active site.[16,17] The second zinc ion (Zn2) has five ligands: an aspartate (Asp86), a cystein (Cys164), a histidine (His206), apical water (Wat2), and Wat1. Kinetic measurements with site-directed mutagenesis showed that a mutation at the zinc-coordinating amino acid residues led to impaired enzymatic activity.[18−20]

Two extended loop regions reside flanking the active site of the CcrA enzyme. The major loop (residues 26−37) constitutes a β-sheet flap, whereas the minor loop (residues 171−178) is situated on the opposite side of the flap about the dizinc center. Dyson and co-workers compared the dynamic properties of the enzyme complexed with a tight binding thiazolidinecarboxylic acid (TCA) inhibitor, 3-[2′-(*S*)-benzyl-3′-mercaptopropanoyl]-4-(*S*)-carboxy-5,5-dimethylthiazolidine (SB225666), to those of the enzyme in the resting form.[21,22] They showed that although loop structures covering the active site had a greater flexibility than the other parts of the enzyme, the motions of these flexible loops were damped out upon binding of the TCA inhibitor. On the basis of these results, the authors argued that the malleability of the loop structures should be responsible for the broad substrate specificity and tight substrate binding. The pivotal role of such loop structures in ligand binding was also observed in mutational analysis of the metallo-β-lactamase IMP-1.[23]

Since the discovery of trifluoromethyl alcohol and ketone,[24] a number of inhibitors for metallo-β-lactamase have been discovered with structural diversity.[25−33] Structure−activity relationship (SAR) studies showed that the derivatives of biphenyl tetrazole (BPT) could be potent inhibitors of the CcrA enzyme with the range of IC_{50} values (0.3−50 μM) depending on a substitution at the 4′-position.[13] It was also found that the ortho position of the tetrazole group relative to the biphenyl ring system should be important in enzyme inhibition, since the movement of the tetrazole group to the meta or para positions led to loss of inhibitory activity. According to the X-ray crystal structure of the enzyme

* To whom correspondence should be addressed. Phone: 814-865-3623. Fax: 814-863-8403. E-mail: merz@psu.edu.

10.1021/jm0491290 CCC: $30.25
Published on Web 02/10/2005

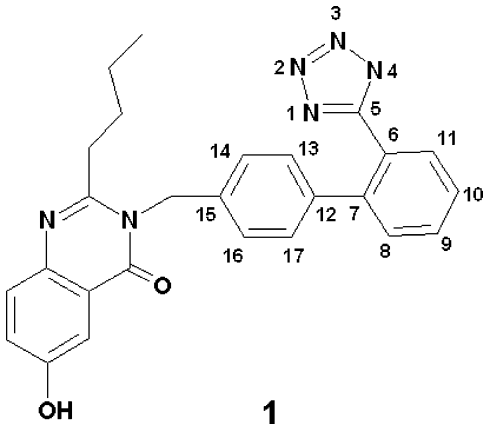

Figure 1. Molecular structure of **1** and the labeling of the biphenyl tetrazole group.

in complex with a biphenyl tetrazole (BPT) inhibitor 2-butyl-6-hydroxy-3-[2′-(1*H*-tetrazol-5-yl)biphenyl-4-ylmethyl]-3*H*-quinazolin-4-one (**1** in Figure 1), the tetrazole ring interacts with active site dizinc center through direct coordination to the second zinc ion, displacing the apical water ligand.[13]

Supplementary to a large amount of experimental work, several theoretical studies on the CcrA enzyme have also been reported in the literature to address the coordination structure of the active site dizinc center,[34−37] the catalytic mechanism,[38,39] and ligand binding.[40−42] In the present study, we investigate the influence of binding of **1** on the dynamic properties of the enzymatic structure on the basis of solution-phase molecular dynamics (MD) simulation. Newly developed force field parameters for zinc ion and its coordination environment are used in the simulations of both apoenzyme and enzyme−inhibitor complex due to the lack of them in the standard force field database. These force field parametrizations are performed with the density functional calculations on the dinuclear zinc clusters modeling the enzymatic active site in the resting form and that complexed with **1**. In these model systems, four imidazole molecules, acetate, and thiolate ions are used to respectively represent four histidine residues (His82, His84, His145, and His206), Asp86, and Cys164 coordinated to active site zinc ions. During the comparative MD study of the CcrA enzyme and its complex with **1**, we focus our interest on clarifying the detailed roles of loop structures flanking the active site in inhibitor binding. We also address the significant binding forces in the enzyme−inhibitor complex by measuring the dynamic stabilities of specific interactions between enzymatic groups and the BPT inhibitor.

Computational Methods

The bonded approach[43,44] was adopted to represent a metal ion with placing explicit bonds between the zinc cation and its ligands, since other nonbonded counterparts have been known to be sensitive to the used electrostatic model, leading to an undesirable coordination geometry.[45,46] To derive the associated force-field parameters that are unavailable in the standard force field database, we followed the procedure suggested by Fox and Kollman[47] to be consistent with the standard AMBER force field.[48] The equilibrium bond lengths and angles for the active site dizinc cluster were taken from the optimized structures of the two model systems representing the active site dizinc cluster of the CcrA enzyme in the resting form and that in complex with **1**. The geometry optimizations were performed at B3LYP/6-31G* level of theory with the Gaussian98 suite of program. The starting coordinates were prepared by extracting atomic coordinates from the X-ray crystal structures of the CcrA enzyme in the resting form (PDB entry 1ZNB) and that in complex with **1** (PDB entry 1A8T). We used the force constant parameters involving the zinc ion from the earlier work of Hoops et al. and Ryde.[43,44] Using the energy-minimized structures, RHF/6-31G* atomic partial charges were derived with electrostatically derived atomic charges[49] through the RESP method[50] to be consistent with the standard AMBER force field. The van der Waals parameters for the zinc ion were taken from the work of Hoops et al.,[43] while those for the atoms in imidazole, carboxylate, thiolate, and BPT groups were assigned from the standard AMBER force field database. We derived the potential parameters for **1** with the same procedure as used for the active-site dizinc clusters, which involves the geometry optimization and charge fitting with the RESP method. Missing force field parameters of the inhibitor were estimated from similar chemical species in the AMBER database.

MD simulations of the CcrA enzyme and its complex with **1** were carried out using the SANDER module of AMBER 6[51] with the force field reported by Cornell et al.[48] The starting coordinates were extracted from X-ray crystal structures of unliganded (PDB entry 1ZNB) and liganded (PDB entry 1A8T) enzymes. The bridging hydroxide ligand missing in the original X-ray structure of the enzyme−inhibitor complex was added on the basis of quantum chemical geometry optimization. The all-atom models for apoenzyme and enzyme−inhibitor complex were neutralized by adding sodium ions and were immersed in rectangular boxes containing 9508 and 9533 TIP3P water molecules, respectively. After 2000 cycles of energy minimization to remove the bad van der Waals contacts, we equilibrated both systems beginning with 20 ps equilibration dynamics of the solvent molecules at 298 K. The next step involved equilibration of the solute with a fixed configuration of the solvent molecules for 5 ps at 10, 50, 100, 150, 200, 250, and 298 K. Then, the equilibration dynamics of the entire system was performed at 298 K for 20 ps. Following the equilibration procedure, 1.05 ns MD simulations were carried out with a periodic boundary condition in the NPT ensemble at 298 K using Berendsen temperature coupling[52] and constant pressure (1 atm) with isotropic molecule-based scaling. The SHAKE algorithm,[53] with a tolerance of 10^{-6}, was applied to fix all bond lengths involving a hydrogen atom. We used a time step of 1.5 fs and a non-bond-interaction cutoff radius of 10 Å; the trajectory was sampled every 0.15 ps (100 step intervals).

Results and Discussion

Force Field Parametrization of the Dinuclear Zinc Clusters. Included in the structural model for the active-site dizinc center are the two crystallographic water molecules (Wat3 and Wat4) that are believed to play a significant role in maintaining the geometry of the active-site dizinc cluster.[37] Indeed, the two structural water molecules reside in close proximity to Wat1 and Wat2 ligands with associated O···O distances of less than 2.9 Å in the high-resolution X-ray structures of the apoenzyme[10] and an enzyme−inhibitor complex in which the inhibitor is bound in the active site without a direct interaction with the two zinc ions.[12] Earlier kinetic studies showed that no ionizable enzymatic group with pK_a values between 5.25 and 10.0 should be involved in the catalytic cycle[54] and that Asp86 would not play a role of proton donor in the enzymatic reaction,[19] implying that Asp86 participates in the enzymatic reaction in its deprotonated form. Further evidence for the ionized Asp86 was provided by recent density functional calculations on a large structural model for the CcrA enzyme.[37] In the force-field parametrization for the dizinc cluster of the CcrA enzyme,

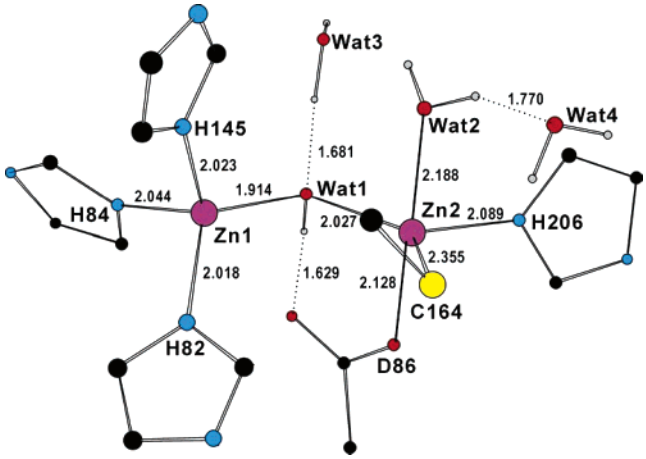

Figure 2. B3LYP/6-31G*-optimized structure of the active site dizinc cluster with ionized Asp86. Selected internuclear distances are given in Å.

therefore, we assume that Asp86 is deprotonated, although the possibility of neutral Asp86 was also proposed on the basis of ab initio calculations on small zinc clusters.[35]

Figure 2 displays the optimized structure for the dizinc center of CcrA enzyme. In accordance with the X-ray crystal structure, Zn1 is tetrahedrally coordinated while Zn2 reveals a trigonal bipyramidal coordination with Asp86 and Wat2 occupying the two axial positions. It is noted that Wat4 accepts a hydrogen bond from Wat2 with an associated O···H distance of 1.77 Å. This interaction may increase the basicity of Wat2 by partial deprotonation, leading to the strengthening of its coordination to Zn2. In contrast, Wat3 donates a hydrogen bond to Wat1. This partial protonation of Wat1 may also play a role in facilitating the Zn2···Wat2 interaction due to the weakening of the Zn1···Wat1 bond with a decreased basicity of Wat1. It is thus likely that the coordination of Wat2 to Zn2 can be stabilized by the cooperative action of Wat3 and Wat4. Apparently, the underestimation of the Zn2···Wat2 interaction in the previous computational studies[34,35] can be attributed to the neglect of the structural roles played by Wat3 and Wat4, exemplifying the importance of the inclusion of these two water molecules in developing the force field parameters of the active site dizinc cluster.

It is noted that in the optimized structure, the RESP atomic charge of the first and the second zinc ions decrease from +2 e to +1.12 e and +0.68 e, respectively. On the other hand, the atomic charges of ligand atoms become less negative by 0.1−0.3 e when compared to those in the standard AMBER force-field database (see the Supporting Information for details). These can be viewed as a reflection of the charge redistribution between the central zinc ions and its ligands upon formation of the metal complex. We used these newly obtained atomic charges in MD simulation, because it has been well-appreciated that the "Zn^{2+}" model with standard force field for ligands is inadequate for maintaining the coordination geometry of an active site zinc complex during the simulations.[45,46]

In the crystal structure of the CcrA enzyme complexed with a BPT derivative, no water molecule was found within a distance of 5.4 Å from the two zinc ions with the Wat2 position being replaced by the tetrazole moiety

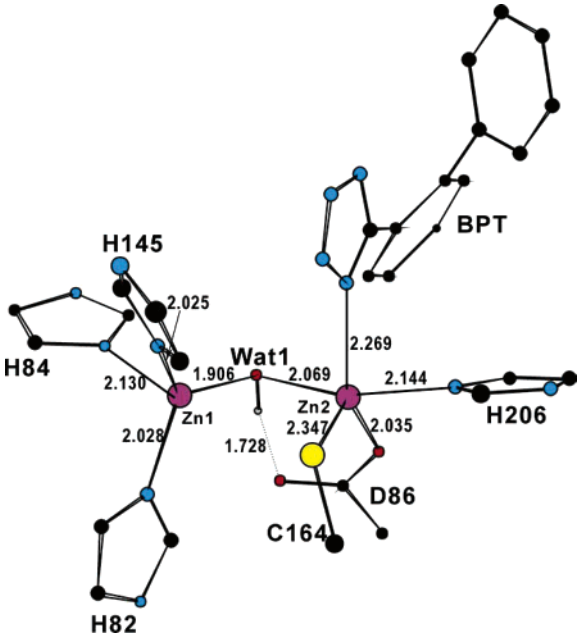

Figure 3. B3LYP/6-31G*-optimized structure of a dinuclear zinc cluster modeling the interaction between the active site of CcrA enzyme and a BPT inhibitor. Selected internuclear distances are given in Å.

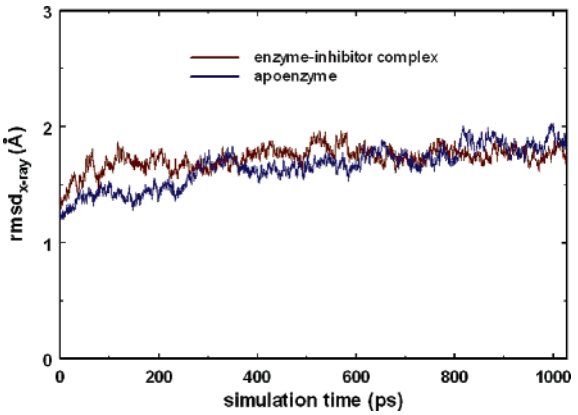

Figure 4. Time dependence of the root-mean-square deviation from the X-ray crystal structure ($rmsd_{X-ray}$) for the apoenzyme (blue) and the enzyme−inhibitor complex (red).

of the inhibitor. Since the bridging hydroxide ligand is believed to play a critical role in stabilizing the dizinc complex, with an associated Zn···Zn distance of less than 3.5 Å, a hydroxide ion (Wat1) was inserted in the middle of the two zinc ions, and its position was optimized with DFT calculations. Figure 3 displays the B3LYP/6-31G*-optimized structure of a model system representing the interaction between the active-site dizinc center including a bridging hydroxide ion and a BPT inhibitor. Similar to the dinuclear zinc cluster of the CcrA in the resting form, Zn1 exhibits a tetrahedral coordination, while Zn2 forms a distorted trigonal bipyramidal complex with five ligands, including the tetrazole moiety of the inhibitor. However, the two axial positions with respect to Zn2 are occupied by Wat1 and His206 side chain, instead of Wat2 and Asp86 as in the apoenzyme.

MD Simulation. Shown in Figure 4 are the root-mean-square deviations from the X-ray crystal structures ($rmsd_{X-ray}$) of all heavy atoms with respect to the simulation time. The $rmsd_{X-ray}$ values remain between

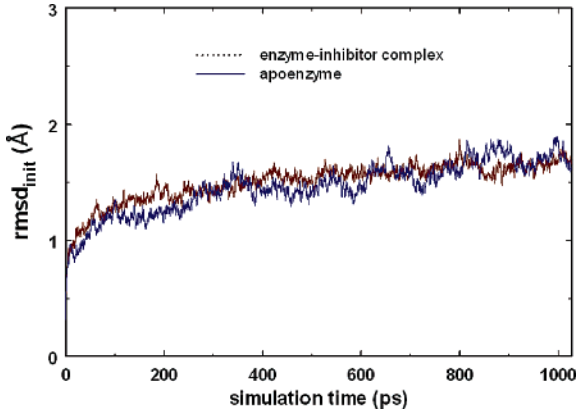

Figure 5. Time dependence of the root-mean-square deviation from the starting structures of production dynamics ($rmsd_{init}$) for the apoenzyme (blue) and the enzyme−inhibitor complex (red).

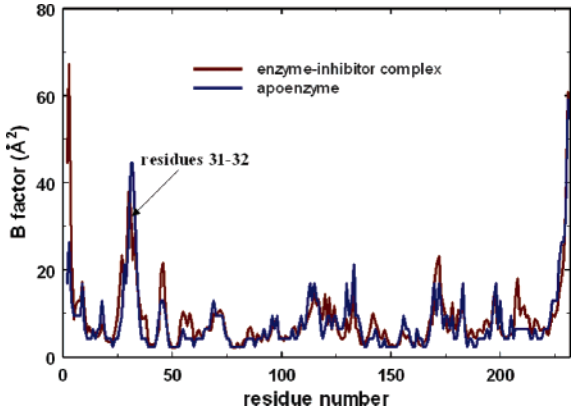

Figure 6. Calculated *B*-factors of the C_α atoms, averaged over 500 ps time frames from 0.55 to 1.05 ns.

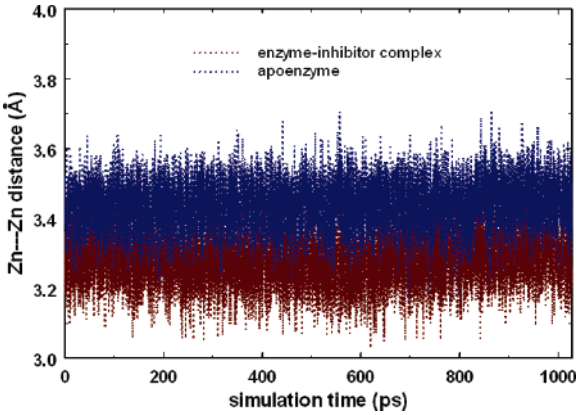

Figure 7. Time evolution of distances between the two active site zinc ions in the apoenzyme (blue) and the enzyme−inhibitor complex (red).

1.2 Å and 2.0 Å for apoenzyme and between 1.3 Å and 2.0 Å for the enzyme−inhibitor complex during the entire course of simulation, indicating that neither unliganded nor liganded enzyme has undergone a significant structural change. Similar to the monozinc metallo-β-lactamase from *B. cereus* and other proteins,[36] the average $rmsd_{X-ray}$ values are found to be 1.5 and 1.6 Å for apoenzyme and the enzyme−inhibitor complex, respectively.

Further evidence for the stability of the protein structure in the course of the simulations may be provided by the time evolution of rmsd from the starting structure of production dynamics ($rmsd_{init}$), which is displayed in Figure 5. The $rmsd_{init}$ values remain within 1.8 Å for both bound and unbound simulations, showing a convergent behavior with respect to the simulation time. Judging from a greater fluctuation of $rmsd_{init}$ values of apoenzyme than those of the enzyme−inhibitor complex, however, the inhibitor binding is likely to increase the rigidity of protein structure.

To estimate the changes in dynamic flexibility of the regions of protein structure due to inhibitor binding, *B*-factors for the C_α atoms (B_i) were calculated using the following relationship:

$$B_i = \frac{8}{3}\pi^2\langle\Delta r_i\rangle^2 \qquad (1)$$

where $\langle\Delta r_i\rangle$ is the rms atomic fluctuation of the C_α atom of residue *i*. As shown in Figure 6, only a few residues show a significant change in the calculated *B*-factor in the presence of **1**. Consistent with the absence of electron density at the apex of the major loop in the X-ray crystal structure (disordered residues Gly31 and Trp32),[10] the calculated *B*-factors for the apoenzyme show a major peak in the region of residues 31 and 32. However, binding of **1** reduces the B_i values for Gly31 and Trp32 by 10.9 and 22.2 Å^2, respectively, suggesting that the motions of these residues are restricted in the enzyme−inhibitor complex. The decrease in dynamic flexibility of the major loop was also observed in NMR relaxation experiments.[22] Differences in the conformational flexibility of the unliganded and liganded proteins can also be estimated by comparing the calculated order parameters of the N−H bond vectors. In this regard, Brooks and co-workers showed that binding of the TCA inhibitor should increase the calculated order parameters of the major loop including residues 31 and 32, indicative of its decreased flexibility in the enzyme−inhibitor complex.[40] Thus, the reduction in the conformational flexibility of the major loop by inhibitor binding can be invoked to explain the potency of tight-binding inhibitors.

Previous X-ray crystallographic[10,11] and computational studies[34] showed that the active site dizinc cluster of the CcrA enzyme exists in both tight and loose forms. To estimate the effects of ligand binding on the size of dizinc center, we calculate the time evolution of the distance between two zinc ions for both bound and unbound simulations. As seen in Figure 7, the Zn···Zn distance of the CcrA−**1** complex remains within 3.03−3.52 Å, as compared to the distance range of 3.16−3.72 Å for apoenzyme. The time-averaged distances of the former and the latter are 3.28 and 3.44 Å, respectively, comparing reasonably well with the mean values of two Zn···Zn distances in the asymmetric unit of their respective crystal structures, 3.03 and 3.47Å.[10,13] It is thus evident that the two active-site zinc ions get closer upon binding of **1**.

Previous ^{15}N NMR relaxation measurements showed that upon binding of a tight-binding thiazolidinecarboxylic acid inhibitor, the loop structures near the active site could undergo a significant change in dynamic flexibility as compared to the rest of enzymatic structure.[22] In particular, a substantial increase of the heteronuclear NOE of the indole moiety of Trp32

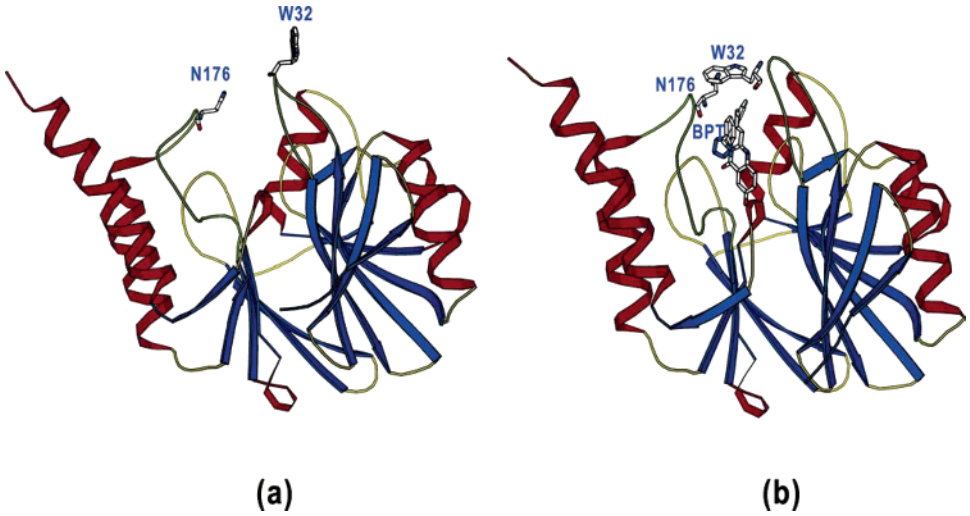

Figure 8. Comparative view of average structures of the 1.05 ns MD simulation for (a) the apoenzyme and (b) the enzyme−inhibitor complex. The positions of the Trp32 and Asn176 are indicated in both structures.

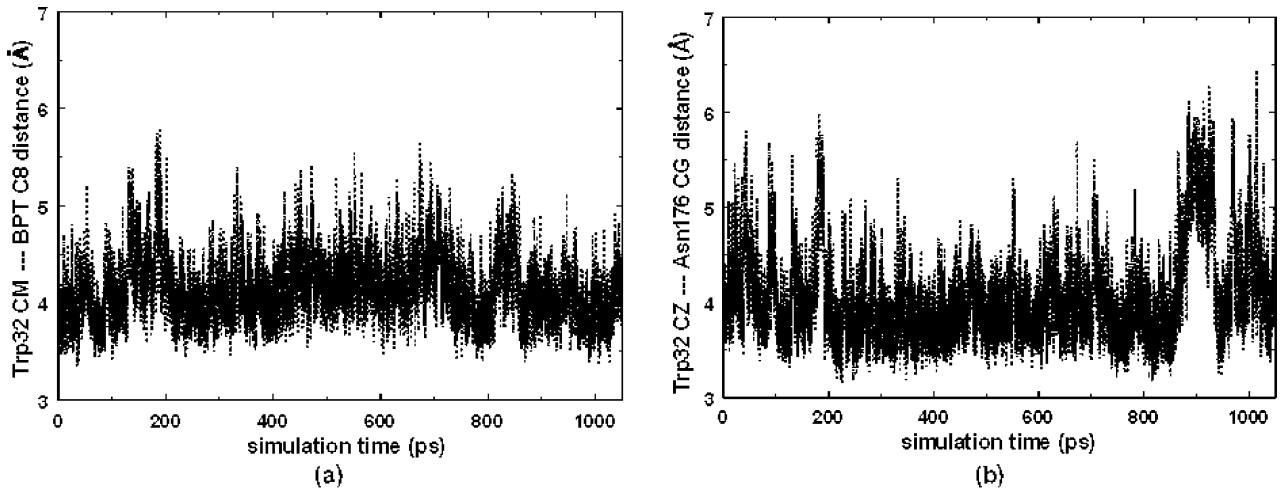

Figure 9. Time evolution of the internuclear distances related with the hydrophobic interactions of Trp32 (a) with **1** and (b) with Asn176.

indicated its significant role in interacting with the inhibitor. We now address the structural change of the loop structures due to binding of **1** and the detailed role of Trp32 in stabilizing the enzyme−inhibitor complex by comparing the conformations of protein molecule in the average structures of bound and unbound MD simulations of the CcrA enzyme. As shown in Figure 8, the active site gorge comprising major and minor loops undergoes a longitudinal elongation and a lateral contraction in the presence of **1**. This observation may be viewed as a support for the previous mechanistic proposal that the broad substrate specificity of the CcrA enzyme could be attributed to the malleability of the loop structures. As will be clarified later, such a conformational change stems from the establishment of hydrophobic interactions between loop residues and the inhibitor. In response to the binding of **1**, the side chain of Trp32 at the apex of the major loop moves toward the minor loop, closing the entrance of the active site gorge in the enzyme−inhibitor complex. As a result, the indole ring of Trp32 forms a face-to-edge interaction with the inhibitor's biphenyl ring and a close van der Waals contact with side chain of Asn176 with an associated Trp32 CZ···Asn176 CG distance of 4.06 Å on average. Thus, the structural features observed in this study are consistent with the previous X-ray crystallographic data in which the side chain of Trp32 of the apoenzyme is localized away from the active site in a solvent-accessible position,[11] whereas it bends toward the active site in enzyme−inhibitor complexes.[12,13]

The stability of the enzyme−inhibitor complex in which the active site gorge is closed by Trp32 may be estimated by examining the time dependence of the interatomic distances associated with hydrophobic interactions of Trp32 with Asn176 and with **1**. As shown in Figure 9, the distance between the center of mass (CM) of the Trp32 side chain indole ring and the C8 atom of the inhibitor remains within 4.50 Å for 87% of the simulation time with average of 4.15 Å. Similarly, the separation between Trp32 CZ and Asn176 CG atoms falls into 4.50 Å for 85% of the simulation time in the enzyme−inhibitor complex, as compared to the average distance of 18.9 Å in the apoenzyme. Thus, the establishment of such hydrophobic interactions can be attributed to the decrease in dynamic flexibility of Trp32 upon binding of **1**. A similar structural change of tryptophan residue in the loop structure was also observed in the IMP-1 metallo-β-lactamase from *P. aeruginosa* in the presence of a mercaptocarboxylic acid inhibitor.[4]

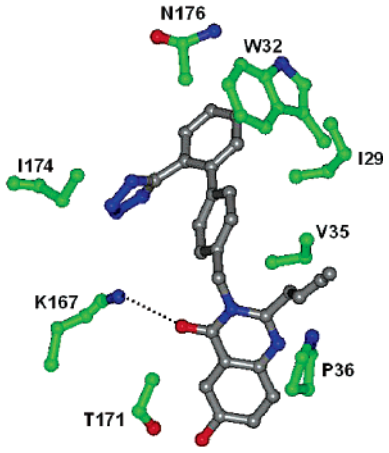

Figure 10. Binding mode of **1** with loop residues and Lys167 in the average structure of the 1.05 ns MD simulation. Carbon atoms belonging to the enzyme and the inhibitor are indicated in green and gray, respectively. A dotted line indicates a hydrogen bond.

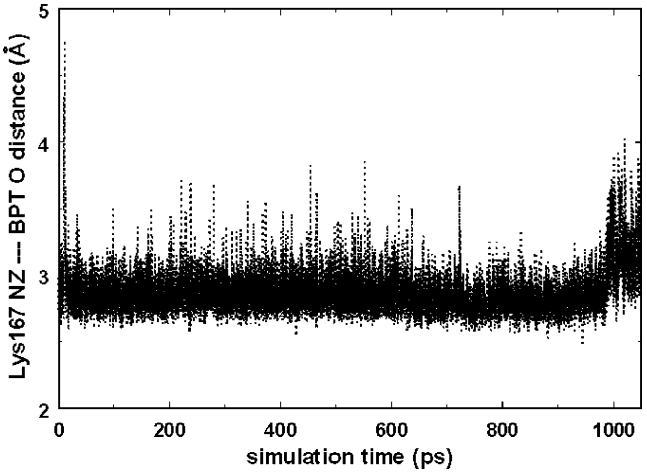

Figure 11. Maintenance of the hydrogen bond between the NZ atom of Lys167 and the inhibitor carbonyl oxygen. The average distance is 2.87 Å.

Depicted in Figure 10 is a schematic of key residues interacting with **1** in the time-averaged structure of the enzyme−inhibitor complex. The inhibitor is bound in the active site through electrostatic and nonpolar interactions. It is seen that both the biphenyl tetrazole ring and the substituent of the inhibitor participate in interacting with the conserved residues of the major loop: the former forms hydrophobic contacts with the side chains of two residues, Trp32 and Ile29, while the latter interacts with Val35 and Pro36. Three residues in the minor loop (Thr171, Ile174, and Asn176) are also in close proximity to the inhibitor, forming the wall of the hydrophobic binding pocket together with side chains of the major loop.

In the X-ray crystal structure of the CcrA enzyme in complex with **1**, the BPT inhibitor forms strong hydrogen bonds only with environmental water molecules. However, the inhibitor carbonyl group points toward the side chain of Lys167 in the average structure of the present solution-phase MD simulation, suggesting the possibility of forming a direct hydrogen bond. To estimate the stability of such a hydrogen bond, we determine the time evolution of the interatomic distance between the Lys167 NZ atom and the carbonyl oxygen of the BPT inhibitor. As can be seen in Figure 11, the hydrogen bond is maintained for 99% of the simulation time when 3.50 Å is the Lys167 NZ···BPT O distance used as a hydrogen-bond-defining distance. Since the inhibitor carbonyl group is situated in the vicinity of the metal binding site (tetrazole ring), such stability of the Lys167 NZ···BPT O hydrogen bond may be viewed as support for the previous mechanistic proposal involving salt bridge formation between the conserved lysine residue and the carboxylate group of a β-lactam substrate.[10,19]

Conclusions

In the optimized geometry of the active-site dinuclear zinc cluster of metallo-β-lactamase CcrA from *B. fragilis* with B3LYP hybrid DFT calculations, the two crystallographic solvent molecules prove to play a significant role in stabilizing the coordination geometry of the dizinc cluster. A 1.05 ns MD simulation with the newly developed force field parameters for the dizinc center shows that binding of **1** causes a reduction of the dynamic flexibility of Gly31 and Trp32 in the major loop as observed in the CcrA enzyme in complex with a tight-binding TCA inhibitor. The active site dinuclear zinc cluster exists in a tighter form in the presence of **1** than the apoenzyme, consistent with previous X-ray crystallographic studies and ab initio calculations. Due to inhibitor binding, the active site gorge comprising major and minor loops undergoes a longitudinal elongation and lateral contraction, supporting the previous experimental implication that the malleability of the loop structures is a significant component of enzyme action. Through the hydrophobic interactions with Asn176 and with the biphenyl ring of **1**, the side chain of Trp32 at the apex of the major loop blocks the entrance of the active site gorge. Such interactions are observed during almost the entire course of our simulation and are believed to play a role in stabilizing the CcrA−**1** complex. The hydrogen bonding of Lys167 to the inhibitor carbonyl group and the hydrophobic interactions between the inhibitor and loop residues are found to be significant interactions in the enzyme−inhibitor complex.

Acknowledgment. We thank the NIH (GM 44974) for generous support of this work.

Supporting Information Available: Modified RESP charges for the active-site dinuclear zinc cluster and its complex with a BPT inhibitor. This material is available free of charge via the Internet at http://pubs.asc.org.

References

(1) Carfi, A.; Pares, S.; Duee, E.; Galleni, M.; Frere, J.-M.; Dideberg, O. The 3-D structure of a zinc metallo-β-lactamase from *Bacillus cereus* reveals a new type of protein fold. *EMBO J.* **1995**, *14*, 4914−4921.

(2) Carfi, A.; Duee, E.; Galleni, M.; Frere, J.-M.; Dideberg, O. 1.85 Å Resolution Structure of the Zn^{II} β-Lactamase from *Bacillus cereus*. *Acta Crystallogr.* **1998**, *D54*, 313−323.

(3) Fabiane, S. M.; Sohi, M. K.; Wan, T.; Payne, D. J.; Bateson, J. H.; Mitchell, T.; Sutton, B. J. Crystal Structure of the Zinc-dependent β-lactamase from *Bacillus cereus* at 1.9 Å resolution: Binuclear active site features of a mononuclear enzyme. *Biochemistry* **1998**, *37*, 12404−12411.

(4) Concha, N. O.; Janson, C. A.; Rowling, P.; Pearson, S.; Cheever, C. A.; Clarke, B. P.; Lewis, C.; Galleni, M.; Frere, J.-M.; Payne, D. J.; Bateson, J. H.; Abdel-Meguid, S. S. Crystal structure of

the IMP-1 metallo-β-lactamase from *Pseudomonas aeruginosa* and its complex with a mercaptocarboxylate inhibitor: Binding determinants of a potent, broad-spectrum inhibitor. *Biochemistry* **2000**, *39*, 4288−4298.
(5) Toney, J. H.; Hammond, G. G.; Fitzgerald, P. M. D.; Sharma, N.; Balkovec, J. M.; Rouen, G. P.; Olson, S. H.; Hammond, M. L.; Greenlee, M. L.; Gao, Y.-D. Succinic acids as potent inhibitors of plasmid-borne IMP-1 metallo-β-lactamase. *J. Biol. Chem.* **2001**, *276*, 31913−31918.
(6) Ullah, J. H.; Walsh, T. R.; Taylor, I. A.; Emery, D. C.; Verma, C. S.; Gamblin, S. J.; Spencer, J. The crystal structure of the L1 metallo-β-lactamase from *Stenotrophomonas maltophilia* at 1.7 Å resolution. *J. Mol. Biol.* **1998**, *284*, 125−136.
(7) McManus-Munoz, S.; Crowder, M. W. Kinetic mechanism of metallo-β-lactamase l1 from S*tenotrophomonas maltophilia*. *Biochemistry* **1999**, *38*, 1547−1553.
(8) Yang, Y.; Keeney, D.; Tang, X.-J.; Canfield, N.; Rasmussen, B. A. Kinetic properties and metal content of the metallo-β-lactamase CcrA harboring selective amino acid substitutions. *J. Biol. Chem.* **1999**, *274*, 15706−15711.
(9) Valladares, M. H.; Felici, A.; Weber, G.; Adolph, H. W.; Zeppezauer, M.; Rossolini, G. M.; Amicosante, G.; Frere, J. M.; Galleni, M. Zn(II) dependence of the *Aeromonas hydrophila* AE036 metallo-β-lactamase activity and stability. *Biochemistry* **1997**, *36*, 11534−11541.
(10) Concha, N. O.; Rasmussen, B. A.; Bush, K.; Herzberg, O. Crystal structure of the wide-spectrum binuclear zinc β-lactamase from *Bacteroides fragilis*. *Structure* **1996**, *4*, 823−836.
(11) Carfi, A.; Duee, E.; Paul-Soto, R.; Galleni, M.; Frere, J.-M.; Dideberg, O. X-ray structure of the Zn^{II} β-lactamase from *Bacteroides fragilis* in an orthorhombic crystal form. *Acta Crystallogr.* **1998**, *D54*, 47−57.
(12) Fitzgerald, P. M. D.; Wu, J. K.; Toney, J. H. Unanticipated inhibition of the metallo-β-lactamase from *Bacteroides fragilis* by 4-morpholineethanesulfonic acid (MES): A crystallographic study at 1.85-Å resolution. *Biochemistry* **1998**, *37*, 6791−6800.
(13) Toney, J. H.; Fitzgerald, P. M. D.; Grover-Sharma, N.; Olson, S. H.; May, W. J.; Sundelof, J. G.; Vanderwall, D. E.; Cleary, K. A.; Grant, S. K.; Wu, J. K.; Kozarich, J. W.; Pompliano, D. L.; Hammond, G. G. Antibiotic sensitization using biphenyl tetrazoles as potent inhibitors of *Bacteroides fragilis* metallo-β-lactamase. *Chem. Biol.* **1998**, *5*, 185−196.
(14) Crowder, M. W.; Wang, Z.; Franklin, S. L.; Zovinka, E. P.; Benkovic, S. J. Characterization of the metal-binding sites of the β-lactamase from *Bacteroides fragilis*. *Biochemistry* **1996**, *35*, 12126−12132.
(15) Throughout this paper, we have followed a numbering scheme that begins at the amino terminus of the 232-residue mature protein, although the sequence of the metallo-β-lactamase from *B. fragilis* contains 249 amino acids.
(16) Eriksson, A. E.; Jones, A. T.; Liljas, A. Refined structure of human carbonic anhydrase II at 2.0 Å resolution. *Proteins* **1988**, *4*, 274−282.
(17) Håkansson, K.; Carlsson, M.; Svensson, L. A.; Liljas, A. Structure of native and apo carbonic anyhdrase II and structure of some of its anion-ligand complexes. *J. Mol. Biol.* **1992**, *227*, 1192−1204.
(18) Li, Z.; Rasmussen, B. A.; Herzberg, O. Structural consequences of the active site substitution Cys181 ⇒ Ser in metallo-β-lactamase from *Bacteroides fragilis*. *Protein Sci.* **1999**, *8*, 249−252.
(19) Yanchak, M. P.; Taylor, R. A.; Crowder, M. W. Mutational analysis of metallo-β-lactamase CcrA from *Bacteroides fragilis*. *Biochemistry* **2000**, *39*, 11330−11339.
(20) Fast, W.; Wang, Z.; Benkovic, S. J. Familial mutations and zinc stoichiometry determine the rate-limiting step of nitrocefin hydrolysis by metallo-β-lactamase from *Bacteroides fragilis*. *Biochemistry* **2001**, *40*, 1640−1650.
(21) Scrofani, S. D. B.; Chung, J.; Huntley, J. J. A.; Benkovic, S. J.; Wright, P. E.; Dyson, H. J. NMR characterization of the metallo-β-lactamase from *Bacteroides fragilis* and its interaction with a tight-binding inhibitor: Role of an active-site loop. *Biochemistry* **1999**, *38*, 14507−14514.
(22) Huntley, J. J. A.; Scrofani, S. D. B.; Osborne, M. J.; Dyson, H. J. Dynamics of the metallo-β-lactamase from *Bacteroides fragilis* in the presence and absence of a tight-binding inhibitor. *Biochemistry* **2000**, *39*, 13356−13364.
(23) Moali, C.; Anne, C.; Lamotte-Brasseur, J.; Groslambert, S.; Devreese, B.; Beeumen, J. V.; Galleni, M.; Frère, J.-M. Analysis of the importance of the metallo-β-lactamase active site loop in substrate binding and catalysis. *Chem. Biol.* **2003**, *10*, 319−329.
(24) Walter, M. W.; Felici, A.; Galleni, M.; Soto, R. P.; Adlington, R. M.; Baldwin, J. E.; Frère, J.-M.; Gololobov, M.; Schofield, C. J. Trifluoromethyl alcohol and ketone inhibitors of metallo-β-lactamases. *Bioorg. Med. Chem. Lett.* **1996**, *6*, 2455−2458.
(25) Tsang, W. Y.; Dhanda, A.; Schofield, C. J.; Frère, J.-M.; Galleni, M.; Page, M. I. The inhibition of metallo-β-lactamase by thioxocephalosporin derivatives. *Bioorg. Med. Chem. Lett.* **2004**, *14*, 1737−1739.
(26) Buynak, J. D.; Chen, H.; Vogeti, L.; Gadhachanda, V. R.; Buchanan, C. A.; Palzkill, T.; Shaw, R. W.; Spencer, J.; Walsh, T. R. Penicillin-derived inhibitors that simultaneously target both metallo- and serine-β-lactamases. *Bioorg. Med. Chem. Lett.* **2004**, *14*, 1299−1304.
(27) Boerzel, H.; Koeckert, M.; Bu, W.; Spingler, B.; Lippard, S. J. Zinc-bound thiolate-disulfide exchange: A strategy for inhibiting metallo-β-lactamases. *Inorg. Chem.* **2003**, *42*, 1604−1615.
(28) Siemann, S.; Clarke, A. J.; Viswanatha, T.; Dmitrienko, G. I. Thiols as classical and slow-binding inhibitors of IMP-1 and other binuclear metallo-β-lactamases. *Biochemistry* **2003**, *42*, 1673−1683.
(29) Walter, M. W.; Valladares, M. H.; Adlington, R. M.; Amicosante, G.; Baldwin, J. E.; Frère, J.-M.; Galleni, M.; Rossolini, G. M.; Schofield, C. J. Hydroxamate inhibitors of *Aeromonas hydrophila* AE036 metallo-β-lactamase. *Bioorg. Chem.* **1999**, *27*, 35−40.
(30) Toney, J. H.; Cleary, K. A.; Hammond, G. G.; Yuan, X.; May, W. J.; Hutchins, S. M.; Ashton, W. T.; Vanderwall, D. E. Structure−activity relationships of biphenyl tetrazoles as metallo-β-lactamase inhibitors. *Bioorg. Med. Chem. Lett.* **1999**, *9*, 2741−2746.
(31) Greenlee, M. L.; Laub, J. B.; Balkovec, J. M.; Hammond, M. L.; Hammond, G. G.; Pompliano, D. L.; Toney, J. H. Synthesis and SAR of thioester and thiol inhibitors of IMP-1 metallo-β-lactamase. *Bioorg. Med. Chem. Lett.* **1999**, *9*, 2549−2554.
(32) Mori, H.; Takahashi, T.; Goto, M.; Ohta, M.; Y. Arakawa, Y. Inhibition of β-lactam hydrolyzing activity of a metallo-β-lactamase by thiol compounds. *J. Inorg. Biochem.* **1997**, *67*, 227.
(33) Walter, M. W.; Adlington, R. M.; Baldwin, J. E.; Schofield, C. J. Synthesis of metallo-β-lactamase inhibitors. *Tetrahedron* **1997**, *53*, 7275−7290.
(34) Gilson, H. S. R.; Krauss, M. Structure and spectroscopy of metallo-lactamase active sites. *J. Am. Chem. Soc.* **1999**, *121*, 6984−6989.
(35) Diaz, N.; Suarez, D.; Merz, K. M., Jr. Zinc metallo-β-lactamase from *Bacteroides fragilis*: A quantum chemical study on model systems of the active site. *J. Am. Chem. Soc.* **2000**, *122*, 4197−4208.
(36) Diaz, N.; Suarez, D.; Merz, K. M., Jr. Molecular dynamics simulations of the mononuclear zinc-β-lactamase from *Bacillus cereus* complexed with benzylpenicillin and a quantum chemical study of the reaction mechanism. *J. Am. Chem. Soc.* **2001**, *123*, 9867−9879.
(37) Peraro, M. D.; Vila, A. J.; Carloni, P. Protonation state of Asp120 in the binuclear active site of the metallo-β-lactamase from *Bacteroides fragilis*. *Inorg. Chem.* **2003**, *42*, 4245−4247.
(38) Olsen, L.; Antony, J.; Ryde, U.; Adolph, H.-W.; Hemmingsen, L. Lactam hydrolysis catalyzed by mononuclear metallo-β-lactamases: A density functional study. *J. Phys. Chem. B* **2003**, *107*, 2366−2375.
(39) Olsen, L.; Rasmussen, T.; Hemmingsen, L.; Ryde, U. Binding of benzylpenicillin to metallo-β-lactamase: A QM/MM Study. *J. Phys. Chem. B* **2004**, *108*, 17639−17648.
(40) Salsbury, F. R., Jr.; Crowley, M. F.; Brooks, C. L., III. Modeling of the metallo-β-lactamase from *B. fragilis*: Structural and dynamic effects of inhibitor binding. *Proteins* **2001**, *44*, 448−459.
(41) Oelschlaeger, P.; Schmid, R. D.; Pleiss, J. Modeling domino effects in enzymes: Molecular basis of the substrate specificity of the bacterial metallo-β-lactamases IMP-1 and IMP-6. *Biochemistry* **2003**, *42*, 8945−8956.
(42) Olsen, L.; Pettersson, I.; Hemmingsen, L.; Adolph, H.-W.; Jorgensen, F. S. Docking and scoring of metallo-β-lactamases inhibitors. *J. Comput.-Aided Mol. Des.* **2004**, *18*, 287−302.
(43) Hoops, S. C.; Anderson, K. W.; Merz, K. M., Jr. Force field design for metalloproteins. *J. Am. Chem. Soc.* **1991**, *113*, 8262−8270.
(44) Ryde, U. Molecular dynamics simulations of alcohol dehydrogenase with a four or five-coordinate catalytic zinc ion. *Proteins* **1995**, *21*, 40−56.
(45) Stote, R. H.; Karplus, M. Zinc binding in proteins and solution: A simple but accurate nonbonded representation. *Proteins* **1995**, *23*, 12−31.
(46) Toba, S.; Colombo, G.; Merz, K. M., Jr. Solvent dynamics and mechanism of proton transfer in human carbonic anhydrase II. *J. Am. Chem. Soc.* **1999**, *121*, 2290−2302.
(47) Fox, T.; Kollman, P. A. Application of the RESP methodology in the parameterization of organic solvents. *J. Phys. Chem B* **1998**, *102*, 8070−8079.
(48) Cornell, W. D.; Cieplak, P.; Bayly, C. I.; Gould, I. R.; Merz, K. M., Jr.; Ferguson, D. M.; Spellmeyer, D. C.; Fox, T.; Caldwell, J. W.; Kollman, P. A. A second generation force field for the simulation of proteins, nucleic acids, and organic molecules. *J. Am. Chem. Soc.* **1995**, *117*, 5179−5197.

(49) Besler, B. H.; Merz, K. M., Jr.; Kollman, P. A. Atomic charges derived from semiempirical methods. *J. Comput. Chem.* **1990**, *11*, 431−439.
(50) Bayly, C. A.; Cieplak, P.; Cornell, W. D.; Kollman, P. A. A well behaved elestrostatic potential based method using charge restraints for deriving atomic charges: The RESP model. *J. Phys. Chem.* **1993**, *97*, 10269−10280.
(51) Case, D. A.; Pearlman, D. A.; Caldwell, J. W.; Cheatham, T. E., III.; Ross, W. S.; Simmerling, C.; Darden, T.; Merz, K. M., Jr.; Stanton, R. V.; Chen, A.; Vincent, J. J.; Crowley, M.; Tsui, V.; Radmer, R.; Duan, Y.; Pitera, J.; Massova, I.; Seibel, G. L.; Singh, U. C.; Weiner, P.; Kollman, P. A. *AMBER 6*; University of California, San Francisco, 1999.
(52) Berendsen, H. C.; Postma, J. P. M.; van Gunsteren, W. F.; DiNola, A.; Haak, J. R. Molecular dynamics with coupling to an external bath. *J. Comput. Phys.* **1984**, *81*, 3684−3690.
(53) Ryckaert, J. P.; Ciccotti, G.; Berendsen, H. C. Numerical integration of the Cartesian equations of motion of a system with constraints: Molecular dynamics of *n*-alkanes. *J. Comput. Phys.* **1977**, *23*, 327−341.
(54) Wang, Z.; Benkovic, S. J. Purification, characterization, and kinetic studies of a soluble *Bacteroides fragilis* metallo-β-lactamase that provides multiple antibiotic resistance. *J. Biol. Chem.* **1998**, *273*, 22402−22408.

JM0491290